

First-Principles Study of the Separation of Am^{III}/Cm^{III} from Eu^{III} with Cyanex301

Xiaoyan Cao,* Daniel Heidelberg, Jan Ciupka, and Michael Dolg*

Institut für Theoretische Chemie, Greinstrasse 4, Universität zu Köln, D-50939 Köln, Germany

Received April 28, 2010

The experimentally observed extraction complexes of trivalent lanthanide Eu^{III} and actinide Am^{III}/Cm^{III} cations with purified Cyanex301 [bis(2,4,4-trimethylpentyl)dithiophosphinic acid, HBTMPDTP denoted as HL], i.e., ML₃ (M = Eu, Am, Cm) as well as the postulated complexes HAmL₄ and HEuL₄(H₂O) have been studied by using energy-consistent 4f- and 5f-in-core pseudopotentials for trivalent f elements, combined with density functional theory and second-order Møller–Plesset perturbation theory. Special attention was paid to explaining the high selectivity of Cyanex301 for Am^{III}/Cm^{III} over Eu^{III}. It is shown that the neutral complexes ML₃, where L acts as a bidentate ligand and the metal cation is coordinated by six S atoms, are most likely the most stable extraction complexes. The calculated metal–sulfur bond distances for ML₃ do reflect the cation employed; i.e., the larger the cation, the longer the metal–sulfur bond distances. The calculated M–S and M–P bond lengths agree very well with the available experimental data. The obtained changes of the Gibbs free energies in the extraction reactions M³⁺ + 3HL → ML₃ + 3H⁺ agree with the thermodynamical priority for Am³⁺ and Cm³⁺. Moreover, the ionic metal–ligand dissociation energies of the extraction complexes ML₃ show that, although EuL₃ is the most stable complex in the gas phase, it is the least stable in aqueous solution.

Introduction

It is well-known that for both actinides (An) heavier than plutonium and lanthanides (Ln) the trivalent oxidation state is most stable in aqueous solution.¹ Because of similar ionic radii, a similar coordination chemistry of Ln^{III} and An^{III} is expected, and chemical separation of the light lanthanides Ln^{III} and the actinides Am^{III}/Cm^{III} becomes difficult in nuclear waste treatment.² In 1995, a very high separation factor (> 5000) between Am^{III} and Eu^{III} was first reported by Zhu and co-workers³ for extraction from the slightly acidic (pH ≈ 3–4) aqueous solution with purified Cyanex301 [bis(2,4,4-trimethylpentyl)dithiophosphinic acid, HBTMPDTP; the acid is denoted hereafter as HL and its anion as L⁻; cf. Figure 1] in kerosene. One year later the corresponding extraction enthalpies and entropies were determined, i.e., 18.10 kJ/mol and –87.10 J/(mol K) for Am and 43.65 kJ/mol and –65.74 J/(mol K) for Eu.⁴ Since then, many experiments have been carried out to study the separation of Ln^{III} and An^{III} by using dithiophosphinic acids and related compounds because of the importance of the separation of transplutonides(III) from lanthanides(III)

in an advanced nuclear fuel cycle.^{5–13} Some experimental studies found that different extraction complexes are formed with dithiophosphinic acids for Ln^{III} and An^{III} and that Ln^{III} preferentially binds to oxygen.^{8–10,12} For example, by using extended X-ray absorption fine structure (EXAFS) spectroscopy, Tian and co-workers found that the structures of the extraction complexes of Am^{III} and Ln^{III} are HAmL₄⁸ and HML₄(H₂O) (M = La, Nd, Eu),⁹ respectively. The determined M–S bond distances for M = Am, La, Nd, and Eu are 2.98,⁸ 3.01,⁹ 2.91,⁹ and 2.84 Å,⁹ respectively. However, Jensen and Bond⁷ have obtained the same extraction complexes ML₃ (M = Cm, Nd, Sm) for lanthanides and actinides, as verified by visible absorption spectroscopy and X-ray absorption fine structure (XAFS) measurements. They have found that the metal–donor atom bond distances are indistinguishable within experimental error bars for similarly sized trivalent lanthanide

*To whom correspondence should be addressed. E-mail: x.cao@uni-koeln.de (X.C.), m.dolg@uni-koeln.de (M.D.). Phone: (00)49-221-470-6893. Fax: (00)49-221-470-6896.

(1) Choppin, G. R. *J. Less-Common Met.* **1983**, *93*, 323.
(2) Dam, H. H.; Reinhoudt, D. N.; Verboom, W. *Chem. Soc. Rev.* **2007**, *36*, 367.
(3) Zhu, Y.; Song, C.; Jiao, R. *Global 95 International Conference on Evaluation of Emerging Nuclear Fuel Cycle System*, Versailles, France, Sept 11–14, 1995; pp 571–576.
(4) Zhu, Y.; Chen, J.; Jiao, R. *Solvent Extr. Ion Exch.* **1996**, *14*, 61.

(5) Chen, J.; Zhu, Y.; Jiao, R. *Sep. Sci. Technol.* **1996**, *31*, 2723.
(6) Modolo, G.; Odoj, R. *J. Radioanal. Nucl. Chem.* **1998**, *228*, 83.
(7) Jensen, M. P.; Bond, A. H. *J. Am. Chem. Soc.* **2002**, *124*, 9870.
(8) Tian, G.; Zhu, Y.; Xu, J.; Hu, T.; Xie, Y. *J. Alloys Compd.* **2002**, *334*, 86.
(9) Tian, G.; Zhu, Y.; Xu, J.; Zhang, P.; Hu, T.; Xie, Y.; Zhang, J. *Inorg. Chem.* **2003**, *42*, 735.
(10) Weigl, M.; Denecke, M. A.; Panak, P. J.; Geist, A.; Gompper, K. *Dalton Trans.* **2005**, *7*, 1281.
(11) Peterman, D. R.; Law, J. D.; Todd, T. A.; Tillotson, R. D. In *Separations for the Nuclear Fuel Cycle in the 21st Century*; Lumetta, G. J., Nash, K. L., Clark, S. B., Fries, J. I., Eds.; ACS Symposium Series 933; American Chemical Society: Washington, DC, 2006; pp 251–259.
(12) Bhattacharyya, A.; Mohapatra, P. K.; Manchanda, V. K. *Solvent Extr. Ion Exch.* **2007**, *25*, 27.
(13) Klähn, J. R.; Peterman, D. R.; Harrup, M. K.; Tillotson, R. D.; Luther, T. A.; Law, J. D.; Daniels, L. M. *Inorg. Chim. Acta* **2008**, *361*, 2522.

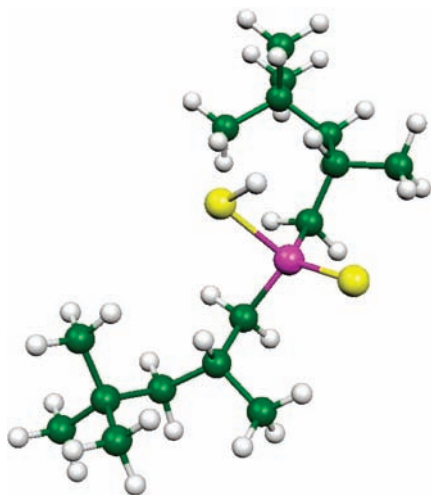


Figure 1. Calculated structure of Cyanex301 (denoted as HL in the text).

and actinide cations;⁷ i.e., the M–S bond lengths for M = Cm, Nd, and Sm are 2.826 ± 0.008 , 2.852 ± 0.007 , and 2.803 ± 0.006 Å, respectively. The origin of the high selectivity of organodithiophosphinic acid ligands for An^{III} cations over Ln^{III} cations has been suggested to be an increased covalence in the An–S bonds that, however, is not reflected in significantly shorter An–S bonds, perhaps because of steric interaction between the ligands or because covalence is only a minor component in both An–S and Ln–S bonding.⁷ In 2007, Bhattacharyya and co-workers¹² studied the dependence of the Am³⁺ (D_{Am}) and Eu³⁺ (D_{Eu}) distribution ratio values on the aqueous-phase pH in the absence of nitrate ions. They found that in both cases the pH dependence follows a slope of ≈ 3 , which indicates extraction of the ML₃ (M = Am and Eu) complexes when the Cyanex301 concentration is higher than 0.3 M.¹²

To our knowledge, there is no theoretical work on the complexation of Ln^{III} and An^{III} ions with Cyanex301 published so far, most likely because of the extremely complex electronic structure of the f elements, where numerous low-lying electronic states, large relativistic effects, and strong electron correlation contributions pose considerable difficulties to theoretical work. However, a few quantum chemical studies comparing lanthanide and actinide complexation by other organic ligands exist, e.g., for polydentate N-donor ligands.^{14–17} Instead of using static quantum chemical calculations as in the present work, liquid–liquid extraction processes may also be modeled by molecular dynamics techniques; cf., e.g., work by Wipff and co-workers on lanthanide cations.^{18,19} Such studies can, e.g., provide insight into the complex processes occurring at the liquid–liquid interface or possible synergistic effects occurring for more than one ligand type. Such topics go beyond the scope of the present work, which mainly concentrates on the relative stability of complexes of selected Ln^{III} and An^{III} ions with Cyanex301 in water as well as in kerosene.

Among the approaches developed in relativistic quantum chemistry, the method of ab initio pseudopotentials (PPs) is one of the most successful ones.²⁰ Because of the core–valence separation, only the chemically relevant valence electron system is treated explicitly and relativistic effects are only implicitly accounted for by a proper adjustment of free parameters in the valence-only model Hamiltonian. Whereas the first aspect leads to a reduction of the computational effort, the second allows inclusion of the scalar relativistic contributions in a nonrelativistic framework. For f elements, relativistic energy-consistent ab initio 4f-in-core^{21,22} and 4f-in-valence²³ PPs were first published in 1989 for lanthanides, and corresponding 5f-in-valence²⁴ PPs for actinides were derived in 1994. During more than 10 years of application in various fields by many researchers, they have been proven to be useful and reliable.^{25,26} However, 5f-in-core^{27,28} actinide PPs became available only in 2007, and thus applications are still scarce.^{29,30}

In this paper, by using 4f-in-core^{21,22} PPs in combination with recently developed basis sets^{21,31} for trivalent lanthanides as well as 5f-in-core²⁸ PPs and corresponding basis sets²⁸ for trivalent actinides, we report a study of the extraction complexes of lanthanides (Eu^{III}) and actinides (Am^{III} and Cm^{III}) with HL at the density functional theory (DFT) level. Additional second-order Møller–Plesset perturbation theory single-point-energy calculations were performed for calibration purposes. Furthermore, solvent effects for water as well as kerosene are taken into account by using the conductor-like screening model (COSMO) approach.³² The structures and stabilities of the extraction complexes, as well as the changes of the Gibbs free energy for complexation in the gas phase and aqueous solution, are discussed. The corresponding Gibbs free energy changes for extraction from the aqueous phase with kerosene are evaluated on the basis of simple assumptions concerning distribution of the involved ions/molecules between the aqueous and organic phases.

Computational Methods

The method of relativistic energy-consistent ab initio PPs is described in detail elsewhere^{21,23,24,27,28} and will be outlined here only briefly. The valence-only model Hamiltonian for a system with n valence electrons and N nuclei with charges Q is given as

$$H_v = -\frac{1}{2} \sum_i^n \Delta_i + \sum_{i < j}^n \frac{1}{r_{ij}} + V_{av} + \sum_{I < J}^N \frac{Q_I Q_J}{r_{IJ}}$$

(20) Kutzelnigg, W. *Phys. Scr.* **1987**, *36*, 416.

(21) Dolg, M.; Stoll, H.; Savin, A.; Preuss, H. *Theor. Chim. Acta* **1989**, *75*, 173.

(22) Dolg, M.; Stoll, H.; Preuss, H. *Theor. Chim. Acta* **1993**, *85*, 441.

(23) Dolg, M.; Stoll, H.; Preuss, H. *J. Chem. Phys.* **1989**, *90*, 1730–1734.

(24) Küchle, W.; Dolg, M.; Stoll, H.; Preuss, H. *J. Chem. Phys.* **1994**, *100*, 7535.

(25) Cao, X.; Dolg, M. *Coord. Chem. Rev.* **2006**, *250*, 900.

(26) Dolg, M.; Cao, X. In *Computational Inorganic and Bioinorganic Chemistry*; Solomon, E. I., King, R. B., Scott, R. A., Eds.; John Wiley & Sons, Ltd.: New York, 2010; in press.

(27) Moritz, A.; Cao, X.; Dolg, M. *Theor. Chem. Acc.* **2007**, *118*, 845.

(28) Moritz, A.; Cao, X.; Dolg, M. *Theor. Chem. Acc.* **2007**, *117*, 473.

(29) Wiebke, J.; Moritz, A.; Cao, X.; Dolg, M. *Phys. Chem. Chem. Phys.* **2007**, *9*, 459.

(30) Cao, X.; Li, Q.; Moritz, A.; Xie, Z.; Dolg, M.; Chen, Y.; Fang, W. *Inorg. Chem.* **2006**, *45*, 3444.

(31) Yang, J.; Dolg, M. *Theor. Chem. Acc.* **2005**, *113*, 212.

(32) Klamt, A.; Schürmann, G. *J. Chem. Soc., Perkin Trans.* **1993**, *2*, 799.

(14) Miguirditchian, M.; Guillauneux, D.; Guillaumont, D.; Moisy, P.; Madić, C.; Jensen, M. P.; Nash, K. L. *Inorg. Chem.* **2005**, *44*, 1404.

(15) Guillaumont, D. *THEOCHEM* **2006**, *771*, 105.

(16) Cao, X.; Dolg, M. *Mol. Phys.* **2003**, *101*, 2427.

(17) Cao, X.; Li, Q.; Moritz, A.; Xie, Z.; Dolg, M.; Chen, Y.; Fang, W. *Inorg. Chem.* **2006**, *45*, 3444.

(18) Diss, R.; Wipff, G. *Phys. Chem. Chem. Phys.* **2005**, *7*, 264.

(19) Coupez, B.; Wipff, G. *C. R. Chim.* **2004**, *7*, 1153.

Here i and j are electron indices and I and J are nuclear indices. In the usual approximation, the molecular PP V_{av} is a superposition of atom-centered PPs

$$V_{av} = \sum_I^N V_{av}^I$$

V_{av}^I denotes a spin-orbit-averaged relativistic PP in a semi-local form for a core I with charge Q_I

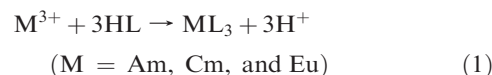
$$V_{av}^I = - \sum_i^n \frac{Q_I}{r_{ii}} + \sum_i^n \sum_{l,k} A_{lk}^I \exp(-a_{lk}^I r_{ii}^2) P_l^I$$

P_l^I is the projection operator on the Hilbert subspace of angular momentum l with respect to center I . The free parameters A_{lk}^I and a_{lk}^I are adjusted to reproduce the valence total energies of a multitude of low-lying electronic states of the neutral atom I and its ions. Large-core PPs for lanthanides^{21,22}/actinides²⁸ have been used; i.e., the 1s-4f/1s-5f shells were included in the PP core, while all others with main quantum numbers larger than 4/5 were treated explicitly (11 valence electrons for Eu, Am, and Cm). The reference data used to determine V_{av} has been taken from all-electron (AE) calculations using the so-called Wood-Boring (WB) scalar-relativistic Hartree-Fock (HF) approach. Both AE WB and PP calculations have been performed with an atomic finite-difference HF scheme in order to avoid basis-set effects in the determination of the PP parameters.

Energy-consistent scalar-relativistic WB-adjusted 52-, 84-, and 85-electron-core PPs were selected for Eu, Am, and Cm, respectively. The corresponding (7s6p5d)/[5s4p3d]^{21,28} standard basis sets for Eu, Am, and Cm were used. All other lighter atoms were treated at the AE level, and the standard def-SV(P) basis sets, as implemented in the *TURBOMOLE*³³ program, were applied, i.e., O (7s4p1d)/[3s2p1d],³⁴ C (7s4p1d)/[3s2p1d],³⁴ H (4s)/[2s],³⁵ S (10s7p1d)/[4s3p1d],³⁴ and P (10s7p1d)/[4s3p1d]³⁴ (denoted hereafter as basis set A). In order to check for possible basis-set deficiencies, larger basis sets were applied too; i.e., a 2f set³¹ was added to the (7s6p5d)/[5s4p3d] basis sets of Eu^{III}²¹ and An^{III}.²⁸ For the lighter elements, def2-TZVP basis sets taken from the basis-set library *TURBOMOLE*³³ were applied, i.e., C (11s6p2d1f)/[5s3p2d1f],³⁶ H (5s1p)/[3s1p],³⁵ S (14s9p3d1f)/[5s5p2d1f],³⁷ and P (14s9p3d1f)/[5s5p2d1f]³⁷ (denoted as basis set B hereafter). Except the above-mentioned two basis sets used for geometry optimizations, the even larger QZVP basis sets were applied too in single-point-energy calculations in order to check the convergence of the results, i.e., C (15s8p3d2f1g)/[7s4p3d2f1g],³⁸ H (7s3p2d1f)/[4s3p2d1f],³⁸ S (20s14p4d2f1g)/[9s6p4d2f1g],³⁸ P (20s14p4d2f1g)/[9s6p4d2f1g],³⁸ a (2f1g)³¹ set added to the (7s6p5d)/[5s4p3d]²¹ basis set of Eu and a (2f1g)²⁸ set to the (7s6p5d)/[5s4p3d]²⁸ basis sets of Am and Cm (denoted as basis set C hereafter).

The experimentally observed extraction complexes of Eu^{III} and An^{III} (An = Am and Cm) with HBTMPDTP (denoted as HL in the following) have been considered, i.e., HAmL₄,⁸ HEuL₄(H₂O),⁹ and ML₃ (M = Am,¹² Cm,⁷ and Eu¹²). The corresponding basic reactions for the extraction

processes can be written as



Whereas the ions M^{3+} and H^+ essentially remain in the aqueous phase, the extraction complexes ML_3 as well as HL mainly reside in the organic (kerosene) phase. As a starting point, all gas-phase molecular structures involved in the above reactions were fully optimized at the DFT level. The change of the Gibbs free energies in aqueous solution, ΔG_s , and for the extraction, ΔG_e , may be obtained by the change of the gas-phase Gibbs free energies, ΔG_g , by adding corrections $\Delta\Delta G_s$ and $\Delta\Delta G_e$, respectively, for solvent effects:

$$\Delta G_{s,e} = \Delta G_g + \Delta\Delta G_{s,e}$$

For example, for reaction (1), one may rewrite ΔG_g and $\Delta\Delta G_{s,e}$ further as

$$\Delta G_g = G_g(ML_3) + 3G_g(H^+) - G_g(M^{3+}) - 3G_g(HL)$$

$$\Delta\Delta G_{s,e} = \Delta G_{sol}(ML_3) + 3\Delta G_{sol}(H^+) - \Delta G_{sol}(M^{3+}) - 3\Delta G_{sol}(HL)$$

Here the subscript "sol" indicates water (hyd) and/or kerosene (org) as the solvent. The gas-phase Gibbs free energies for ML_3 , H^+ , HL, and M^{3+} , i.e., $G_g(ML_3)$, $G_g(H^+)$, $G_g(HL)$, and $G_g(M^{3+})$, are determined from the total gas-phase energy by adding the zero-point energy and a thermal correction by using the ideal gas model for $T = 298.15$ K and $p = 0.1$ MPa. The hydration Gibbs free energies for ML_3 and HL, i.e., $\Delta G_{hyd}(ML_3)$ and $\Delta G_{hyd}(HL)$, were approximated by single-point-energy calculations for fixed gas-phase molecular structures by addressing bulk solvation effects with the COSMO approach.³² Whereas for $\Delta G_{hyd}(H^+)$ and $\Delta G_{hyd}^-(Eu^{3+})$ experimental data exist (H^+ , -1104.5 kJ/mol;³⁹ Eu^{3+} , -3364.1 kJ/mol⁴⁰), this does not seem to be the case for $\Delta G_{hyd}(Am^{3+})$ and $\Delta G_{hyd}(Cm^{3+})$. In order to be able to compare the complex formation and extraction for Eu^{III} with those for Am^{III} and Cm^{III}, we rely on recently published results from quantum chemical calculations (Eu^{3+} , -3152.0 kJ/mol;⁴¹ Am^{3+} , -2994 kJ/mol;²⁹ Cm^{3+} , -3027 kJ/mol²⁹ all for coordination number 9 and derived for a monomer cycle⁴¹) as well as on semiempirical data (Eu^{3+} , -3252.2 kJ/mol;⁴² Am^{3+} , -3159 kJ/mol;⁴³ Cm^{3+} , -3225 kJ/mol⁴³). We note that, e.g., coordination number 8 instead of 9 for Eu^{3+} corresponds to an about 20 kJ/mol more negative $\Delta G_{hyd}^-(Eu^{3+})$ value,⁴¹ and values derived from the preferred cluster cycle are about 100 kJ/mol more negative⁴¹ but not available for actinides.²⁹

The ionic metal-ligand dissociation energies, ΔE_{diss} , for the extraction complexes ML_3 (M = Eu, Am, and Cm) were

(39) Tissandier, M. D.; Cowen, K. A.; Feng, W. Y.; Gundlach, E.; Cohen, M. H.; Earhart, A. D.; Tuttle, T. R.; Coe, J. V. *J. Phys. Chem. A* **1998**, *102*, 7787.

(40) Goldman, S.; Morss, L. R. *Can. J. Chem.* **1975**, *53*, 2695.

(41) Ciupka, J.; Cao, X.; Wiebke, J.; Dolg, M. *Phys. Chem. Chem. Phys.* **2010**, DOI: 10.1039/C0CP00639D.

(42) David, F. H.; Vokhmin, V.; Ionova, G. *J. Mol. Liq.* **2001**, *90*, 45.

(43) David, F. H.; Vokhmin, V. *New J. Chem.* **2003**, *27*, 1627.

(33) *TURBOMOLE* is a program package developed by the Quantum Chemistry Group at the University of Karlsruhe, Germany, since 1988: Ahlrichs, R.; Bär, M.; Häser, M.; Horn, H.; Kölmel, C. *Chem. Phys. Lett.* **1989**, *162*, 165.

(34) Schäfer, A.; Horn, H.; Ahlrichs, R. *J. Chem. Phys.* **1992**, *97*, 2571.

(35) Unpublished; *TURBOMOLE* basis set library.

(36) Weigend, F.; Häser, M.; Patzelt, H.; Ahlrichs, R. *Chem. Phys. Lett.* **1998**, *294*, 143.

(37) Weigend, F.; Ahlrichs, R. *Phys. Chem. Chem. Phys.* **2005**, *7*, 3297.

(38) Weigend, F.; Furche, F.; Ahlrichs, R. *J. Chem. Phys.* **2003**, *119*, 12753.

calculated according to the dissociation paths, which most likely are preferred in aqueous solution; i.e., $\Delta E_{\text{diss}} = E(\text{M}^{3+}) + 3E(\text{L}^-) - E(\text{ML}_3)$ ($\text{M} = \text{Eu}, \text{Am}, \text{and Cm}$). In analogy with the calculations of ΔG , the energies of M^{3+} , L^- , and ML_3 in aqueous solution, i.e., $E(\text{M}^{3+})$, $E(\text{L}^-)$, and $E(\text{ML}_3)$, are approximated by single-point-energy calculations for fixed gas-phase molecular structures by accounting for bulk solvation effects with the COSMO approach.³² On the basis of the ML_3 geometry data, ΔG_{S} and ΔE_{diss} , the covalence in the M–L bonds, as well as the high selectivity of Cyanex301 for An^{III} over Ln^{III} , will be discussed.

Most of the calculations have been carried out at the DFT level with the *TURBOMOLE* program package.^{33,44} The generalized gradient approximation (GGA) type density functional BP86 was applied; i.e., the Hartree–Fock exchange energy is approximated by using the gradient-corrected exchange-energy functional proposed by Becke⁴⁵ in 1988, and the electron correlation energy is approximated by using the DFT proposed by Perdew⁴⁶ in 1986. Calculations taking into account hydration effects were carried out using COSMO,³² where the dielectric constant for water was used, $\epsilon = 80$. Solvation effects for kerosene were calculated correspondingly using $\epsilon = 1.8$. COSMO is a variant of the continuum solvation model, which uses a scaled conductor boundary condition for calculation of the polarization charges of a molecule (solute) in a continuum (solvent). For the cavity generation, the following atomic radii (Å) were used in our COSMO calculations: C, 1.989; H, 1.404; O, 1.7784; S, 2.106; P, 2.106; Eu, 1.820; Am, 2.045; Cm, 2.020. The values for Eu, Am, and Cm were chosen to reproduce within about 4 kJ/mol (1 kcal/mol) accuracy the experimental (Eu^{3+} , -3364.1 kJ/mol⁴⁰) and calculated (Am^{3+} , -2994 kJ/mol;²⁹ Cm^{3+} , -3027 kJ/mol²⁹) hydration Gibbs free energies for $[\text{An}^{\text{III}}(\text{OH}_2)_9]^{3+}$ ($\text{An} = \text{Am}$ and Cm). It has been found for the Ln^{III} water complexes that the actual choice of the radius for the metal cation does not influence the calculated energies unless an artificially high value is used so that the Ln^{III} cavity sphere extends beyond those spanned by the surrounding atoms. For all other elements, the default values implemented in *TURBOMOLE* were adopted.

Additional single-point-energy calculations were performed using the resolution of the identity second-order Møller–Plesset perturbation theory approach (RI-MP2)⁴⁷ implemented in *TURBOMOLE*,³⁵ and the local MP2 approach (LMP2)⁴⁸ as well as the spin-component scaled variant (SCS-MP2)⁴⁹ implemented in *MOLPRO*⁵⁰ for calibrating the electronic energy contributions derived at the DFT level.

Results and Discussion

Structures of Extraction Complexes ML_3 ($\text{M} = \text{Eu}, \text{Am}$, and Cm ; $\text{HL} = \text{HBTMPDTP}$). The most important parameters of the optimized structures, as well as available experimental data, are listed in Table 1. Additional information is provided in the Supporting Information. Let us first check the performance of the applied basis sets. Two basis sets were used for geometry optimizations: i.e., basis set A, def-SV(P) for C, H, S, and P and standard (7s6p5d)/[5s4p3d] valence basis sets for Eu, Am, and Cm; basis set B, def2-TZVP for C, H, S, and P and standard (7s6p5d)/[5s4p3d] valence basis sets augmented by (2f)

Table 1. Selected Averaged Bond Lengths (Å) and Averaged Bond Angles (deg) for ML_3 ($\text{M} = \text{Eu}, \text{Am}$, and Cm ; $\text{HL} = \text{HBTMPDTP}$) Calculated at the DFT/BP86 Level in Comparison with Available Experimental Data (in Parentheses)^{a,7}

	Eu	Am	Cm
$R(\text{M}-\text{S})$	2.863/2.841	2.918/2.900	2.900/2.883 (2.826 ± 0.008)
$R(\text{M}-\text{P})$	3.454/3.420	3.502/3.479	3.483/3.461 (3.45 ± 0.01)
$R(\text{S}-\text{P})$	2.059/2.038	2.060/2.039	2.060/2.039
$R(\text{P}-\text{C})$	1.864/1.851	1.865/1.852	1.865/1.852
$\angle \text{SMS}$	73.03/72.96	72.0/71.7	72.4/72.1
$\angle \text{SPS}$	111.7/112.0	112.7/112.8	112.6/112.7
$\angle \text{CPC}$	99.38/99.1	99.90/99.2	99.9/99.3
$\angle \text{PSMS}$	3.46/3.45	0.1/0.4	0.0/0.3

^a ... refers to the results obtained by using basis sets A and B; i.e., A, def-SV(P) for C^{34} (7s4p1d)/[3s2p1d], H^{35} (4s)/[2s], O^{34} (7s4p1d)/[3s2p1d], S^{34} (10s7p1d)/[4s3p1d], and P^{34} (10s7p1d)/[4s3p1d] and standard (7s6p5d)/[5s4p3d] valence basis sets for Eu,²¹ Am,²⁸ and Cm;²⁸ B, def2-TZVP for C^{36} (11s6p2d1f)/[5s3p2d1f], H^{35} (5s1p)/[3s1p], S^{37} (14s9p3d1f)/[5s5p2d1f], and P^{37} (14s9p3d1f)/[5s5p2d1f] and standard (7s6p5d)/[5s4p3d] valence basis sets augmented by a (2f) set for Eu^{21,31} and a (2f) set for Am²⁸ and Cm.²⁸ For basis sets A and B, 52-, 84-, and 85-electron-core PPs were selected for Eu, Am, and Cm, respectively.

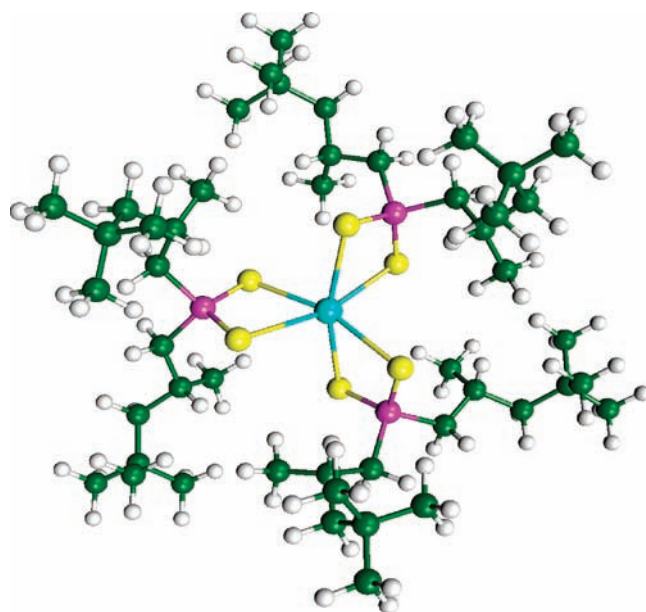


Figure 2. Calculated ML_3 ($\text{M} = \text{Eu}^{3+}, \text{Am}^{3+}$, and Cm^{3+} ; $\text{L} = \text{R}_2\text{PS}_2^-$; $\text{R} = 2,4,4\text{-trimethylpentyl}$) structure with C_3 symmetry.

sets for $\text{M} = \text{Eu}, \text{Am}$, and Cm . The application of both basis sets leads to C_3 symmetry of the ML_3 complexes as determined from the results of geometry optimizations within C_1 and C_3 symmetry (cf. Figure 2). Compared to the results obtained with the basis set A, the calculated bond distances decrease only slightly by using the larger basis set B; i.e., the average differences are 0.018, 0.027, 0.021, and 0.013 Å for the M–S, M–P, S–P, and P–C bonds, respectively. Bond angles are even less affected by the application of different basis sets; i.e., the differences for the bond angles are less than 1°. For the discussion below, the results for the basis set B are used, which we assume to be fairly close to the basis-set limit in the case of geometries.

The Am and Cm atoms are found to be located in the plane defined by the two S atoms and the one P atom belonging to the same ligand, whereas Eu is situated slightly above this plane; i.e., the dihedral angle of M–S–S–P is 3.5°, 0.4°, and 0.3° for $\text{M} = \text{Eu}, \text{Am}$, and

(44) Treutler, O.; Ahlrichs, R. *J. Chem. Phys.* **1995**, *102*, 346.

(45) Becke, A. D. *Phys. Rev. A* **1988**, *38*, 3098.

(46) Perdew, J. P. *Phys. Rev. B* **1986**, *33*, 8822.

(47) Weigend, F.; Häser, M. *Theor. Chem. Acc.* **1997**, *97*, 331.

(48) Schütz, M.; Hetzer, G.; Werner, H.-J. *J. Chem. Phys.* **1999**, *111*, 5691.

(49) Grimme, S. *J. Chem. Phys.* **2003**, *118*, 9095.

(50) *MOLPRO* is a package of ab initio programs written by: Werner, H.-J.; Knowles, P. J.; et al.; version 2009.1.

Table 2. Mulliken Orbital Populations (s, p, d, and f) and Atomic Charges (Q) on the Metal Center M (M = Eu, Am, and Cm), P, and S in the Extraction Complexes ML_3 (HL = HBTMPDTP)^a

	s	p	d	f	Q
Eu	2.36	6.40	1.29	0.02	0.94
P	5.46	8.46	0.61	0.04	0.42
S	5.91	10.47	0.07	0.01	-0.45
S	5.90	10.45	0.07	0.01	-0.42
Am	2.39	6.15	1.18	0.07	1.21
P	5.46	8.51	0.62	0.04	0.37
S	5.90	10.49	0.07	0.01	-0.46
S	5.90	10.47	0.07	0.01	-0.45
Cm	2.40	6.16	1.18	0.06	1.20
P	5.46	8.51	0.62	0.04	0.37
S	5.90	10.48	0.07	0.01	-0.46
S	5.90	10.47	0.07	0.01	-0.45

^a Basis set B (cf. Table) for C, H, S, and P and 52-, 84-, and 85-electron-core PPs and corresponding standard (7s6p5d)/[5s4p3d] valence basis sets augmented by a (2f) set for Eu, Am, and Cm.

Cm, respectively. The M–S distances do reflect the size of M^{3+} ; i.e., the Cm–S and Eu–S bond lengths are shorter than the Am–S bond length by 0.017 and 0.059 Å, respectively, in agreement with the decreasing ionic radius of Am^{3+} (1.115 Å), Cm^{3+} (1.110 Å), and Eu^{3+} (1.087 Å) (cf. Table 1). We note that, besides the M^{3+} ionic radii, the M–S distances are also determined by the steric interaction, including Pauli repulsion, between the ligands as well as possible covalent contributions to bonding. Our calculated bond distances and angles excluding the central ions are almost not affected by the substitution of the metal; e.g., the variations of the S–P and P–C bond lengths are at most 0.002 and 0.001 Å, respectively. Compared to the available experimental data obtained by Jensen and Bond⁷ for CmL_3 by visible absorption spectroscopy and XAFS measurements, the calculated bond lengths of Cm–S (2.883 Å) and Cm–P (3.461 Å) are only 0.057 and 0.011 Å longer than the experimental values [$R(Cm-S) = 2.826 \pm 0.008$ Å and $R(Cm-P) = 3.45 \pm 0.01$ Å; cf. Table 1].

The Mulliken orbital populations (cf. Table 2) show small charge populations in the f symmetry for Eu (0.02), Am (0.07), and Cm (0.06). We note that the f-in-core PPs applied for the metals in this work contribute six (Eu), six (Am), and seven (Cm) f electrons to the core but allow for slightly higher nonintegral f occupations by means of a modified f projector.^{21,22,28} The additional f populations for Am and Cm are slightly higher than that for Eu because of the more diffuse character of the 5f orbitals compared to the 4f orbitals, which is mainly because of the stronger f shell destabilization and expansion by the indirect relativistic effects for the heavier actinides as well as the compact nature of the lanthanide f shell due to missing orthogonality constraints to the inner shells of the same angular momentum. This might imply a very weak participation in the bonding of the actinide 5f shells. Significant 5d, 6s, and 6p occupations; i.e., 5d, 1.29, 1.18, 1.18; 6s, 0.36, 0.39, 0.40; 6p, 0.40, 0.15, 0.16 electrons for Eu, Am, and Cm, respectively, are observed for all complexes, indicating covalent metal–ligand bonding contributions from these shells; i.e., substantial deviations from a purely ionic complex between M^{3+} [f^m]s²p⁶ and L^- are found.

The degree of covalence in the An^{III} –S bonds was considered to be greater than that in the Ln^{III} –S bonds, which might lead to shorter An–S bonds.⁷ Our calculated results do not confirm this expectation; i.e., longer M–S bonds for An^{III} were obtained: $R(Eu-S) = 2.841$ Å, $R(Am-S) = 2.900$ Å, and $R(Cm-S) = 2.883$ Å. Note that the calculated bond distance difference $R(Cm-S) - R(Eu-S) = 0.042$ Å agrees very well with the experimentally observed difference $R(Cm-S) - R(Sm-S) = 0.023$ Å,⁷ corrected with the difference between the Sm^{3+} and Eu^{3+} ionic radii (1.098 – 1.087 = 0.012 Å), i.e., an estimated experimental value of $R(Cm-S) - R(Eu-S) = 0.035$ Å. We find that the Mulliken charges on Am (1.21) and Cm (1.20) are even larger than those on Eu (0.94); e.g., AmL_3 and CmL_3 appear to be more ionic than EuL_3 , which is mainly because of the higher p and d populations on Eu. It should be noted that EuL_3 is slightly (by ≈ 50 –100 kJ/mol) more tightly bound in the gas phase with respect to the ions Eu^{3+} and L^- than it is for AmL_3 and CmL_3 (cf. below). In order to check the reliability of our results obtained with f-in-core PPs and DFT methods, we performed ab initio calculations on model molecules, i.e., trivalent metal dihydrogen sulfide complexes, $EuSH_2^{3+}$ and $AmSH_2^{3+}$ by using f-in-valence PPs²⁴ combined with configuration interaction methods. Here the Am–S bond is found to be 0.041 Å longer than the Eu–S bond. Moreover, the Mulliken charge distributions on the atoms do not show a significant difference between the Eu–S and Am–S bonds, i.e., $Eu^{2.51+S^{0.08-}}$ and $Am^{2.51+S^{0.06-}}$. It should be mentioned that, for the ground states of EuS ($8\sum^-4f^7\sigma^2\sigma^2\pi^4$) and AmS ($8\sum^-5f^7\sigma^2\sigma^2\pi^4$), the Am–S bond is found to be as short as the Eu–S bond, i.e., $R(Eu-S) = 2.410$ Å and $R(Am-S) = 2.408$ Å, and the atomic charges show a slightly increased covalence in the Am–S bond, i.e., $Am^{0.90+S^{0.90-}}$ vs $Eu^{1.00+S^{1.00-}}$. The conclusions drawn from our model systems, however, have to be viewed with some care because in MSH_2^{3+} the overall charge is different from that in ML_3 , whereas for MS, it is the oxidation state of the metal.

Structures of Extraction Complexes $HAmL_4$ and $HEuL_4(H_2O)$ (HL = HBTMPDTP). The structurally identical ML_3 extraction complexes with Cyanex301 for both Ln^{III} and An^{III} , where the metal is bound to six S atoms, were experimentally studied by visible absorption spectroscopy and XAFS by Jensen and Bond.⁷ Besides, these differently 8-fold-coordinated trivalent lanthanide and actinide cations were also reported by other experimentalists, i.e., $HAmL_4$, where Am is bound to eight S atoms from four BTMPDTP ligands,⁸ and $HEuL_4(H_2O)$, where Eu is bound by seven S atoms from four BTMPDTP ligands and one O atom from a hydrated water.⁹ It was suggested that the composition and structural differences of the extraction complexes may be one of the most important factors for the high selectivity of Cyanex301 for Am^{III} over Eu^{III} .⁹ Because DFT geometry optimizations using small basis sets are already very time-consuming (e.g., about 10^3 geometry optimization steps and several CPU weeks) for systems with several long, flexible, and sterically interacting alkyl chains such as in HML_4 or $HML_4(H_2O)$, we performed only exploratory calculations using basis set A with starting geometries based on the results for small model systems (cf. below) as well as based on the above suggestions for the composition and structure.

Although because of the basis-set deficiencies we cannot provide reliable energetic estimates for relative stabilities, we believe that our structural results still provide some useful hints.

It has been found that in aqueous solution Eu^{3+} , Am^{3+} , and Cm^{3+} prefer an 8-to-9-fold coordination in hydration complexes.^{29,41,51–53} Because the atomic radius of S (0.88 Å⁵⁴) is almost twice the atomic radius of O (0.48 Å⁵²), one might expect that the M^{3+} ions do not get stabilized by eight S atoms because of a stronger steric hindrance. Nevertheless, it has been found in crystal structures that tetrakis-8-fold-coordinate anionic complexes MX_4^- are formed for some lanthanide M^{3+} ions ($\text{M} = \text{La}, \text{Ce}, \text{Nd}, \text{Ho}, \text{and Er}$) as well as MX_4 for Th^{4+} with dithiophosphinate ligands, $\text{X} = \text{R}_2\text{PS}_2$, however, only when R is relatively small (OMe, OPr^t, and Et).^{55,56} Boehme and Wipff performed quantum chemical studies for phosphate and dithiophosphinate complexes for some lanthanide M^{3+} ions ($\text{M} = \text{La}, \text{Eu}, \text{and Yb}$) and found a 7-fold coordination for $\text{MX}_3(\text{HX})$ for $\text{X} = \text{R}_2\text{PS}_2$ and $\text{R} = \text{Me}$ at the Hartree–Fock level, applying the same lanthanide 4f-in-core PPs as those used here.⁵⁷ Because in several studies DFT approaches were found to be biased to yield lower coordination numbers,^{58,59} we performed DFT/BP86 geometry optimizations with basis set A for MX_3 , HMX_4 , $\text{HMX}_4(\text{H}_2\text{O})$, and MX_4^- ($\text{M} = \text{Eu}$ and Am) with the same ligand X as that used by Boehme and Wipff. In agreement with their results, we found a 7-fold coordination for HMX_4 , which exhibits an intramolecular hydrogen bond between the S–H group and the S atom of a neighboring X ligand. As expected, we found coordination numbers 6 and 8 in MX_3 and MX_4^- , respectively. However, a complex $\text{HMX}_4(\text{H}_2\text{O})$ with 8-fold (or higher) coordination (to seven or eight S atoms and one O atom) was not found to be stable. The optimizations rather yielded $\text{MX}_3(\text{H}_2\text{O})(\text{HX})$ with 7-fold coordination (six S atoms and one O atom) by four ligands (three X and a H_2O) and HX in the second coordination sphere, bonded by three hydrogen bonds ($\text{O}-\text{H}\cdots\text{S}$, $\text{O}-\text{H}\cdots\text{SH}$, and $\text{S}\cdots\text{H}-\text{S}$). Slightly less stable structures $\text{HMX}_4(\text{H}_2\text{O})$ exhibit also only 7-fold metal coordination (six S atoms and one O atom), however by five ligands (three X, a HX, and a H_2O) and three hydrogen bonds ($\text{O}-\text{H}\cdots\text{S}$, $\text{O}-\text{H}\cdots\text{SH}$, and $\text{S}\cdots\text{H}-\text{S}$); however, HX and one X ligand are each bound with only one S atom directly to the metal, whereas the other two X ligands coordinate with two S atoms to the metal.

Our calculations on small models for the extraction complexes rule out metal coordination numbers of 8

(or higher) and rather favor 7-fold metal coordination. Going back to Cyanex301, we note that Jensen and Bond⁷ pointed out that the EXAFS data could be fitted equally well by models with 6- and 8-fold metal coordination. Thus, they based their assignment of 6-fold metal coordination and ML_3 complexes on the known absorption spectrum of NdL_3 in toluene.⁷ Grigorieva et al.⁶⁰ recently summarized that frequently contradictory experimental results for the extraction complexes of Cyanex301 exist and gave Ni^{2+} as an example, where depending on the extraction conditions five different complexes were reported. Our calculations for complexes with the composition HML_4 ($\text{M} = \text{Eu}, \text{Am}$) indicate that only 7-fold metal coordination exists, with the S–H group of HL forming a hydrogen bond to a S atom on a neighboring ligand. Almost at the same energy, we find structures that rather correspond to ML_3 with 6-fold metal coordination and that HL in the second coordination sphere only bonded to a S atom of one of the ligands L in the first coordination sphere by a hydrogen bond ($\text{S}\cdots\text{H}-\text{S}$). However, both structures are still slightly higher in energy than the separated ML_3 and HL systems, probably mainly because of steric interactions between the bulky alkyl chains. Calculations of higher accuracy are needed in order to decide if HML_4 , $\text{ML}_3(\text{HL})$, or merely ML_3 are relevant for the extraction.

For complexes with the composition $\text{HML}_4(\text{H}_2\text{O})$, we find that H_2O is always directly coordinated to the metal in ML_3 . HL and one ligand L are coordinated with only one S atom to the metal, whereas the other ligands complex the metal with two S atoms, resulting in 7-fold metal coordination. Two hydrogen bridges ($\text{O}-\text{H}\cdots\text{S}$ and $\text{S}\cdots\text{H}-\text{S}$) are formed, i.e., one between H_2O and the free S atom of the singly coordinated ligand L and one between the S–H group of HL and the metal-coordinated S atom of the singly coordinated ligand L. The complexes, which are clearly more stable than their fragments $\text{ML}_3 + \text{H}_2\text{O} + \text{HL}$, thus correspond to $\text{HML}_3(\text{H}_2\text{O})$. Again, higher level calculations are needed to establish reliable estimates for the stabilities.

We thus conclude that, according to our present DFT/BP86 results, HAmL_4 and $\text{HEuL}_4(\text{H}_2\text{O})$ with 8-fold (or higher) metal coordination are probably not stable extraction complexes. We also did not observe any significantly different behavior of Eu^{III} and Am^{III} ; i.e. from our exploratory calculations, we have no indication that different extraction complexes are formed by the two metals. Therefore, also considering the computer resources at our hands, in the discussion below, only the most simple extraction complexes ML_3 and the related extraction processes are considered.

Change of the Gibbs Free Energy, ΔG_s , for $\text{M}^{3+} + 3\text{HL} \rightarrow \text{ML}_3 + 3\text{H}^+$ ($\text{M} = \text{Eu}, \text{Am}, \text{Cm}$; $\text{HL} = \text{HBTMPDTP}$). For the titled reactions, the changes in the Gibbs free energy, $\Delta G_{s,e} = \Delta G_g + \Delta \Delta G_{s,e}$, were calculated for the gas phase (ΔG_g), for an aqueous solution (ΔG_s), and for extraction from the aqueous phase by using kerosene (ΔG_e). For the convenience of the discussion, we partition the gas phase (ΔG_g) and solvent ($\Delta \Delta G_{s,e}$) contributions further. The gas-phase Gibbs free energy change ΔG_g is

(51) Ishiguro, S.; Umabayashi, Y.; Komiya, M. *Coord. Chem. Rev.* **2002**, *226*, 103.

(52) Yang, T.; Bursten, B. *Inorg. Chem.* **2006**, *45*, 5291.

(53) Yamaguchi, T.; Nomura, M.; Wakita, H.; Ohtaki, H. *J. Phys. Chem.* **1988**, *89*, 5153.

(54) Clementi, E.; Raimondi, D. L.; Reinhardt, W. P. *J. Chem. Phys.* **1967**, *47*, 1300.

(55) Pinkerton, A. A.; Schwarzenbach, D.; Spiliadis, S. *Inorg. Chim. Acta* **1987**, *128*, 283.

(56) Spiliadis, S.; Pinkerton, A. A.; Schwarzenbach, D. *Inorg. Chim. Acta* **1983**, *75*, 115.

(57) Boehme, C.; Wipff, G. *Eur. J. Chem.* **2001**, *7*, 1398.

(58) Rotzinger, F. P. *J. Phys. Chem. B* **2005**, *109*, 1510.

(59) Austin, J. P.; Burton, N. A.; Hillier, I. H.; Sundararajan, M.; Vincent, M. A. *Phys. Chem. Chem. Phys.* **2009**, *11*, 1143.

(60) Grigorieva, N. A.; Pavlenko, N. I.; Pleshkov, M. A.; Pashkov, G. L.; Fleitikh, I. Yu. *Solvent Extr. Ion. Exch.* **2009**, *27*, 745.

split into an electronic contribution and one arising from vibration, rotation, and translation:

$$\Delta G_g = \Delta G_g^{\text{elec}} + \Delta G_g^{\text{vib+rot+trans}}$$

The two contributions are evaluated as follows:

$$\Delta G_g^{\text{elec}} = E^{\text{elec}}(\text{ML}_3, \text{g}) - 3E^{\text{elec}}(\text{HL}, \text{g}) - E^{\text{elec}}(\text{M}^{3+}, \text{g})$$

$$\begin{aligned} \Delta G_g^{\text{vib+rot+trans}} &= G_g^{\text{vib+rot+trans}}(\text{ML}_3) \\ &- 3G_g^{\text{vib+rot+trans}}(\text{HL}) - G_g^{\text{trans}}(\text{M}^{3+}) + 3G_g^{\text{trans}}(\text{H}^+) \end{aligned}$$

Note that $E^{\text{elec}}(\text{H}^+, \text{g}) = 0$ and thus has been omitted. The corrections due to the solvents (water and kerosene) are also split into two parts:

$$\Delta \Delta G_{s,e} = \Delta \Delta G'_{\text{sol}} + \Delta \Delta G''_{\text{sol}}$$

The neutral and unpolar extraction complexes ML_3 as well as Cyanex301 HL reside for the extraction mainly in the organic (kerosene) phase (sol = org) but are also considered in the aqueous phase (sol = hyd), whereas the atomic ions H^+ and M^{3+} are only considered in the aqueous phase:

$$\Delta \Delta G'_{\text{sol}} = \Delta G_{\text{sol}}(\text{ML}_3) - 3\Delta G_{\text{sol}}(\text{HL})$$

$$\Delta \Delta G''_{\text{sol}} = 3\Delta G_{\text{sol}}(\text{H}^+) - \Delta G_{\text{sol}}(\text{M}^{3+})$$

Thus, it follows for our model calculations of the Gibbs free energies of hydration and extraction:

$$\Delta G_e = \Delta G_s - \Delta \Delta G'_{\text{hyd}} + \Delta \Delta G'_{\text{org}}$$

The accurate evaluation of ΔG_s and ΔG_e is hindered by several difficulties and uncertainties, which are well-known but cannot be completely removed at present. The gas-phase electronic contribution ΔG_g^{elec} evaluated at the PP DFT level might not be accurate enough because of both the PP and the applied BP86 functional. Whereas calibration studies for the PPs point to relatively small errors,²⁸ mainly also because the metals stay in their stable M^{3+} state, one might question the accuracy of the DFT approach. We were able to perform RI-MP2 calculations using *TURBOMOLE*³³ as well as LMP2 and SCS-LMP2 calculations using *MOLPRO*⁴⁹ for basis set B. The results listed in Table 3 indicate a quite strong dependence of the absolute values on the computational scheme, whereas the trends as measured by corresponding differences for two elements appear to be quite stable. Similarly, it was also found that smaller basis sets yield quite different absolute LMP2 results, whereas the trends remain essentially unchanged. Our largest calculations comprised more than 2200 basis functions in C_1 symmetry and involved considerable computational effort. Higher level coupled-cluster studies would be highly desirable in order to derive more accurate absolute values but are beyond our current computational capacity. A similar statement holds for the hydration contributions $\Delta G_{\text{hyd}}(\text{M}^{3+})$, which were also determined at the BP86 DFT level.^{29,41} Although these contributions agree within 4–7% with the corresponding semiempirical values^{42,43}

Table 3. Calculated Change in the Electronic Gibbs Free Energy Contribution, ΔG_g^{elec} (kJ/mol), in the Reactions $\text{M}^{3+} + 3\text{HL} \rightarrow \text{ML}_3 + 3\text{H}^+$ (M = Eu, Am, and Cm; HL = HBTMPDTP) and Corresponding Differences^a

	DFT/BP86	RI-MP2	LMP2	SCS-LMP2
Eu	29.1	−187.1	−161.3	−69.3
Am	118.7	−66.7	−28.1	60.8
Cm	85.0	−102.7	−62.1	27.5
Eu → Am	89.6	120.4	133.2	130.0
Eu → Cm	55.9	84.3	99.2	96.8
Am → Cm	−33.7	−36.0	−34.0	−33.3

^a Basis set B (cf. Table 1).

and are within 7% of the experimental value for Eu^{3+} hydration,⁴⁰ the relatively small errors of both data sets still may amount to more than 100 kJ/mol and enter directly into the theoretical results for ΔG_s and ΔG_e . The explicit consideration of the second hydration sphere would possibly yield more reliable results but is computationally very demanding.

Uncertainties arise not only from the applied quantum chemical method but also from details on how the quantities in the underlying thermodynamic cycles are evaluated, e.g., if n H_2O monomers or a $(\text{H}_2\text{O})_n$ cluster, both using the *COSMO*³² approach for bulk hydration effects, are considered as references for $\text{M}(\text{H}_2\text{O})_n^{3+}$ complexes.⁴¹ It is also not clear if HBTMPDTP is to be considered as a monomer ML, a dimer $(\text{ML})_2$, or a mixture thereof containing also higher oligomers.⁶⁰ These uncertainties affect all three metals equally and any error/approximation leads to a shift in the absolute ΔG_s values. Even if we assume that all other calculated ($\Delta G_g^{\text{vib+rot+trans}}$) and experimental contributions [$\Delta G_{\text{hyd}}(\text{H}^+)$] are sufficiently accurate, the discussed sources of error only leave some hope to obtain reasonable trends for the three metals, but not for very accurate absolute ΔG_s and ΔG_e values.

By using a monatomic ideal gas model, the gas-phase Gibbs free energies for Eu^{3+} , Am^{3+} , Cm^{3+} , and H^+ at 1 atm and 298.15 K are evaluated by using the Sackur–Tetrode equation, i.e., $G_g^{\text{trans}}(\text{M}^{3+})$ (M = Eu, Am, and Cm) are −44.9, −46.7, and −46.7 kJ/mol for M = Eu, Am, and Cm, respectively, and $G_g^{\text{trans}}(\text{H}^+)$ is −26.3 kJ/mol. The components of ΔG_s and ΔG_e calculated with basis sets A and B are listed in Table 4. In the gas phase using basis set B, the calculated changes in the Gibbs free energy for formation of the ML_3 complexes according to reaction (1) (ΔG_g) are 63.6, 143.1, and 109.9 kJ/mol for Eu, Am, and Cm, respectively. Formation of the ML_3 complexes according to reaction (1) is thus endothermic, with EuL_3 being less unstable than AmL_3 and CmL_3 .

The quality of the basis sets, especially the metal f functions, is found to have quite big effects on the electronic energy; i.e., ΔG_g^{elec} increases by about 90 kJ/mol when going from basis set A to basis set B, whereas $\Delta G_g^{\text{rot+vib+trans}}$ increases only by 17–24 kJ/mol. We note that a further increase of the basis set quality does not lead to significant changes; e.g., single-point calculations using the QZVP basis set C based on the optimized structure obtained by using basis set B show that the obtained results of ΔG_g^{elec} are only further increased by at most 10 kJ/mol.

By taking into account the solvent effects, we found that contributions from the hydration energies of the HL and ML_3 (M = Eu, Am, Cm) complexes $\Delta \Delta G'_{\text{hyd}}$ increase by at most 10 kJ/mol when going from basis set A

Table 4. Calculated Change in the Components ΔG_g and $\Delta\Delta G_{s,e}$ (kJ/mol) of the Gibbs Free Energy $\Delta G_{s,e}$ for the Reactions $M^{3+} + 3HL \rightarrow ML_3 + 3H^+$ ($M = \text{Eu, Am, and Cm}$; HL = HBTMPDTP) in the Gas Phase and an Aqueous Solution and for Extraction with Kerosene^a

	ΔG_g		$\Delta\Delta G_{s,e}$		
	ΔG_g^{elec} A/B/C	$\Delta G_g^{\text{vib+rot+trans}}$ A/B	$\Delta\Delta G'_{\text{hyd}}$ A/B	$\Delta\Delta G'_{\text{org}}$ A/B	$\Delta\Delta G''_{\text{hyd}}$ calcd/estd
Eu	-64.2/29.1/33.2	10.6/34.5	23.5/33.9	7.3/10.0	-162.1/-61.3
Am	31.4/118.7/128.7	6.3/24.4	26.2/34.2	7.9/9.9	-319.5/-154.5
Cm	-4.1/85.0/95.3	7.6/24.9	26.2/34.8	7.9/10.1	-286.5/-88.5

^a .../(...) refers to the results obtained with basis sets A/B/C (cf. Table 1) for ΔG_g , $\Delta\Delta G'_{\text{hyd}}$, and $\Delta\Delta G'_{\text{org}}$ and to quantum chemically derived^{29,41} (calcd) as well as semiempirically estimated^{42,43} (estd) values for $\Delta\Delta G''_{\text{hyd}}$ of M^{3+} . For H^+ , the experimental value $\Delta G_{\text{hyd}}(H^+) = -1104.5$ kJ/mol³⁹ was used in both cases. For the definition of the entries, compare the text. Dielectric constants: water, 80 (hyd); kerosene, 1.8 (org).

Table 5. Calculated Change of the Gibbs Free Energy ΔG_s for the Reactions $M^{3+} + 3HL \rightarrow ML_3 + 3H^+$ ($M = \text{Eu, Am, and Cm}$; HL = HBTMPDTP) in Aqueous Solution^a

	ΔG_s		ΔG_e	
	$\Delta\Delta G''_{\text{hyd}}$ (calcd) A/B	$\Delta\Delta G''_{\text{hyd}}$ (estd) A/B	$\Delta\Delta G''_{\text{hyd}}$ (calcd) A/B	$\Delta\Delta G''_{\text{hyd}}$ (estd) A/B
Eu	-192.2/-64.6	-91.4/36.2	-208.4/-88.5	-107.6/12.3
Am	-255.6/-142.2	-90.6/22.8	-273.9/-166.5	-108.9/-1.5
Cm	-256.8/-141.8	-58.8/56.5	-275.1/-166.5	-77.1/31.5

^a Corresponding estimated values ΔG_e for extraction with kerosene are also listed. .../(...) refers to the results obtained with basis sets A/B (cf. Table 1) for ΔG_g , $\Delta\Delta G'_{\text{hyd}}$, and $\Delta\Delta G'_{\text{org}}$. Quantum chemically derived^{29,41} (calcd) as well as semiempirically estimated^{42,43} (estd) values for $\Delta\Delta G''_{\text{hyd}}$ of M^{3+} were used. For H^+ , the experimental value $\Delta G_{\text{hyd}}(H^+) = -1104.5$ kJ/mol³⁹ was used in both cases. For the definition of the entries, compare the text.

to basis set B and are almost identical for Eu (33.9 kJ/mol), Am (34.2 kJ/mol), and Cm (34.8 kJ/mol). A similar finding applies to the $\Delta\Delta G'_{\text{org}}$ values for the kerosene phase, which are about a factor of 3 smaller.

Qualitatively, the values for the hydration contributions of the M^{3+} and H^+ cations $\Delta\Delta G_{\text{hyd}}''$ exhibit the same trends for the quantum chemically calculated M^{3+} hydration Gibbs free energies^{29,41} and the semiempirically determined ones;^{42,43} however, the absolute values for a given metal differ by 100–200 kJ/mol. These contributions clearly favor complex formation for Am and Cm over the one for Eu and revert the trend of ΔG_g determined mainly by ΔG_g^{elec} . The more negative Gibbs free hydration energy for Eu^{3+} compared to Am^{3+} and Cm^{3+} appears therefore to be the decisive contribution for the observed preference of Cyanex301 for complex formation with the actinides rather than with the lanthanides.

Table 5 finally lists the Gibbs free energies ΔG_s for reaction (1) $M^{3+} + 3HL \rightarrow ML_3 + 3H^+$ ($M = \text{Eu, Am, and Cm}$; HL = HBTMPDTP) in aqueous solution as well as ΔG_e for extraction with kerosene. For the latter case, the slightly endothermic experimental values may be estimated for 298.15 K to be 44.1 kJ/mol for Am and 63.3 kJ/mol for Eu.⁴ Because the actual reaction mechanism of the extraction process, which probably occurs mainly at the boundary between the aqueous and organic phases (cf., e.g., ref 61 for Cyanex302), is too complex to be studied by quantum chemical methods, we only try to model the situations before (M^{3+} in water) and after (ML_3 in kerosene) extraction and omit the kinetic aspects. It is worthwhile to mention here that it has been found by Modolo and Odoj⁶² that at room temperature the extraction equilibrium for Am^{III} over Eu^{III} by using purified Cyanex301 was already attained within 5 min.⁵⁸ ΔG_e for the extraction is consistently lower than ΔG_s for the aqueous solution, in agreement with the experimental

finding that ML_3 and HL mainly reside in the kerosene phase. The results for basis set B obtained with semiempirical values for the Am^{3+} and Eu^{3+} Gibbs free hydration energies, i.e. 12.3 kJ/mol for Eu and -1.5 kJ/mol for Am, agree quite favorably with these. On the basis of the results for ΔG_g^{elec} (Table 4), one might even speculate that basis set C would yield about 10 kJ/mol higher values in even better agreement with the experimental findings. However, there is evidence that Cyanex301 in organic solvents such as nonane is not only present as a monomer HL but forms dimers $(HL)_2$ and tetramers $(HL)_4$ via S–H–S hydrogen bonds.⁶⁰ Assuming a similar behavior for kerosene and using a calculated dimerization energy of 10.9 kJ/mol (16.1 kJ/mol in the gas phase and -1.6 kJ/mol in water), the ΔG_e values relying on the semiempirical M^{3+} Gibbs free hydration energies discussed above would become slightly endothermic (Eu, 28.7 kJ/mol; Am, 14.9 kJ/mol) in quite good agreement with the values (Eu, 63.3 kJ/mol; Am, 44.1 kJ/mol) obtained for 298.15 K from experimental data.⁴ However, the value for Cm is found to be more endothermic than the one for Eu, which does not agree with the expectation that it should be close to the one for Am. Although the trend of the purely theoretical results also agrees with the experimental finding, especially the large difference of ≈ 80 kJ/mol between the Eu value and those for Am and Cm is not satisfactory.

Stability of ML_3 ($M = \text{Eu, Am, and Cm}$; HL = HBTMPDTP). The ionic metal–ligand binding energies for ML_3 ($M = \text{Eu, Am, and Cm}$) were calculated according to the dissociation path $ML_3 \rightarrow M^{3+} + 3L^-$, which are most likely preferred in aqueous solution:

$$\Delta G_g^{\text{elec}} = E^{\text{elec}}(ML_3, g) - 3E^{\text{elec}}(L^-, g) - E^{\text{elec}}(M^{3+}, g)$$

$$\Delta\Delta G_{\text{hyd}} = G_{\text{hyd}}(ML_3) - 3G_{\text{hyd}}(L^-) - G_{\text{hyd}}(M^{3+})$$

The calculated DFT BP86 ionic gas-phase binding energies $\Delta E_{\text{diss}} = -\Delta G_g^{\text{elec}}$ for basis set B (Eu, 4046.3 kJ/mol; Am, 3956.8 kJ/mol; Cm, 3990.5 kJ/mol) reflect a trend $\text{Eu} > \text{Cm} > \text{Am}$ similar to that of the M^{3+} Gibbs free

(61) Abdel Rahman, N.; Daoud, J. A.; Aly, H. F. *J. Radioanal. Nucl. Chem.* **2003**, *25*, 597.

(62) Modolo, G.; Odoj, R. *J. Radioanal. Nucl. Chem.* **1998**, *228*, 83.

hydration energies $-\Delta G_{\text{hyd}}$ (Eu, 3152.0 kJ/mol;⁴¹ Am, 2994 kJ/mol;²⁹ Cm, 3027 kJ/mol²⁹). However, whereas the Eu^{3+} hydration energy is by 158 and 125 kJ/mol higher than those of Am^{3+} and Cm^{3+} , respectively, the hydration energies of the ML_3 complexes are very similar (EuL₃, 38.8 kJ/mol; AmL₃, 38.5 kJ/mol; CmL₃, 37.8 kJ/mol). Because the ionic EuL₃ gas-phase binding energy is only 89 and 54 kJ/mol higher than those of AmL₃ and CmL₃, respectively, the relatively high Eu^{3+} hydration energy renders EuL₃ to be the most unstable of the three ML_3 extraction complexes in aqueous solution. Calculating $\Delta\Delta G_{\text{hyd}}$ for the aqueous solution entirely with the *COSMO* approach, one obtains stabilities $-\Delta G_{\text{s}}$ of ML_3 with respect to M^{3+} and L^- of 54.2, 334.4, and 330.4 kJ/mol for Eu, Am, and Cm, respectively, also supporting this view.

From the discussions above, we found that the hydration energies for Eu^{III} , Am^{III} , and Cm^{III} have played an important role in the energy balance of the extraction reactions for $\text{Am}^{\text{III}}/\text{Cm}^{\text{III}}$ by using Cyanex301, i.e., because of the higher hydration energies for Eu^{III} compared to those for Am^{III} and Cm^{III} , the extraction reactions for $\text{Am}^{\text{III}}/\text{Cm}^{\text{III}}$ by using Cyanex301 in aqueous solution are preferred and the extraction complexes AmL₃/CmL₃ are more stable than EuL₃. Although the hydration energies for Am^{III} and Cm^{III} applied in our calculations are only approximate values because accurate experimental hydration energies for them are still unavailable, we want to point out that, to the best of our knowledge, all available data in the literature show a higher hydration energy ($-\Delta G$) for Eu^{III} than for Am^{III} and Cm^{III} , i.e., Eu^{3+} , 3364.1⁴⁰ and 3252.2 kJ/mol;⁴² Am^{3+} , 2994²⁹ and 3159 kJ/mol;⁴³ Cm^{3+} 3027²⁹ and 3225 kJ/mol.⁴³ The big differences in the results of different methods listed above reflect the difficulties in getting accurate values for ΔG for charged solutes. Correlated ab initio reference calculations of trivalent lanthanide and actinide aquo ions should be done in the future in order to obtain a more consistent data set.

Conclusions

The experimentally observed extraction complexes of M^{III} (M = Eu, Am, and Cm) with Cyanex301 (HL = HBTMPDTP), i.e., HAmL_4 , $\text{HEuL}_4\cdot\text{H}_2\text{O}$, and ML_3 , were calculated using the DFT/BP86 method in connection with scalar-relativistic energy-consistent 4f/5f-in-core lanthanide/actinide PPs. For the postulated extraction complexes with the composition HAmL_4 and $\text{HEuL}_4(\text{H}_2\text{O})$, the metal cations were supposed to be 8-fold-coordinated; however, at least at the applied DFT/BP86 level, at most a 7-fold metal coordination was found, e.g., HAmL_4 or $\text{AmL}_3(\text{HL})$ with 7- and 6-fold coordination, respectively, and $\text{HEuL}_4(\text{H}_2\text{O})$ with a 7-fold

metal coordination. For the neutral bidentate extraction complexes ML_3 , where the metal cation is coordinated by six S atoms with no water molecules in the inner coordination sphere, the M–S bond distances do reflect the cation employed; i.e., the larger the cation, the longer the bond. The calculated M–S/M–P bond lengths (i.e., EuL₃, 2.841/3.420 Å; AmL₃, 2.900/3.479 Å; CmL₃, 2.883/3.461 Å) agree well with available experimental data [$R(\text{Cm–S}) = 2.826 \pm 0.008$ Å; $R(\text{Cm–P}) = 3.45 \pm 0.01$ Å]. The changes of the Gibbs free energy, ΔG , in the reactions $\text{M}^{3+} + 3\text{HL} \rightarrow \text{ML}_3 + 3\text{H}^+$ in the gas phase and aqueous solution and for extraction from aqueous solution with kerosene have been studied too. It has been found that the hydration Gibbs free energies for M^{3+} play an important role for the high selectivity of Cyanex301 for Am^{III} and Cm^{III} over Eu^{III} ; i.e., in the gas phase, the calculated values of ΔG_{g} for Eu^{3+} (63.6 kJ/mol) are smaller than those for Am^{3+} (143.1 kJ/mol) and Cm^{3+} (109.9 kJ/mol), whereas this order is reverted for the aqueous solution (ΔG_{s} : Eu, –64.6 kJ/mol; Am, –142.2 kJ/mol; Cm, –141.8 kJ/mol) as well as for the extraction (ΔG_{e} : Eu, –88.5 kJ/mol; Am, –166.5 kJ/mol; Cm, –166.5 kJ/mol). Replacing quantum chemically calculated Gibbs free hydration energies for Eu^{3+} and Am^{3+} by semiempirically estimated values, we obtain for the extraction values of 12.3 and –1.5 kJ/mol, respectively. If Cyanex301 is assumed to form dimers $(\text{HL})_2$ in kerosene, the absolute values for the extraction are slightly increased to 28.7 and 14.9 kJ/mol, in qualitative agreement with the experimental findings (Eu, 63.3 kJ/mol; Am, 44.1 kJ/mol). The extraction complex EuL₃ is concluded to be more stable than AmL₃ and CmL₃ based on the calculated ionic metal–ligand gas-phase binding energies (Eu, 4046.6 kJ/mol; Am, 3956.9 kJ/mol; Cm, 3990.6 kJ/mol), but because of the higher hydration Gibbs free energies for Eu^{3+} compared to Am^{3+} and Cm^{3+} , it is the most unstable extraction complex in the aqueous solution. Accurate correlated ab initio reference calculations as well as further experiments on trivalent lanthanide and actinide aquo ions should be done in the future in order to get more accurate values for M^{3+} hydration Gibbs free energies, and thus also more reliable data for evaluation of the energetics of the Cyanex301 complexation and extraction processes. In addition, extraction complexes other than ML_3 should be investigated in more detail.

Acknowledgment. We thank Prof. J. Chen for bringing the topic of $\text{An}^{\text{III}}/\text{Ln}^{\text{III}}$ separation by using Cyanex301 to our attention and for valuable discussions, as well as his hospitality during X.C.'s visit to his group.

Supporting Information Available: Additional information concerning the optimized structures. This material is available free of charge via the Internet at <http://pubs.acs.org>.